



# Self-Calibrating Stress Measurement System Based on Multidirectional Barkhausen Noise Measurements

Leszek Piotrowski<sup>1</sup> · Marek Chmielewski<sup>1</sup>

Received: 20 August 2024 / Accepted: 11 October 2024 / Published online: 22 October 2024  
© The Author(s) 2024

## Abstract

The system presented in this paper enables automatization of the two-dimensional calibration process (determination of Barkhausen noise (BN) intensity dependence on in-plane components of strain). Then, using dedicated software created by the authors in LabVIEW environment, and with the help of two dimensional calibration data one can effectively determine strain and stress distribution i.e. magnitude and orientation of main strain/stress components relative to measurement direction. BN signal measurements are performed using an advanced, multidirectional Barkhausen noise (BN) measuring sensor and a measurement system dedicated for cooperation with it. The system uses a robust algorithm for the strain components determination based on calibration surfaces, instead of usually applied curves, thus taking the influence of normal strain component directly into account instead of treating it as a correction factor (if not completely neglecting). The originality of the system arises also from the fact that this is the first BN measurement system that is self-calibrating (i.e. automatically loads the calibration sample in a pre-programmed way, performs BN signal measurements and calculates calibration planes), provided that the user possesses enough of the investigated material for calibration sample preparation.

**Keywords** Barkhausen noise · Strain measurement · Stress · Nondestructive evaluation

## 1 Introduction

Determination of stress distribution on the surface of the investigated material can be an important factor, responsible for the integrity of the manufactured product, as well as for ensuring the safety of many industrial components in operation. One of the ways of strain/stress determination is the use of Barkhausen noise (BN) measurements [1–4]. The BN signal is generated during intermittent movement of magnetic domain walls (DW) which get pinned and unpinned at material imperfections such as precipitates grain boundaries and dislocation tangles. The unpinned DW jumps to the next pinning location and as a result of magnetic flux modification caused by the jump an electromagnetic pulse is generated. This pulse can be detected by the pick-up coil if it is generated close enough (down to ~ 1 mm) to the surface. Otherwise it gets completely attenuated due to local eddy current generation. Since DW structure in ferromagnetic materials is

modified by the external and residual strain/stress the BN signal is also modified thus enabling finding correlation between measured signal and in plane strain distribution.

The authors of this article undertook the task of creating a fully self-sufficient measurement set, using the Barkhausen effect in order to effectively determine the stress distribution on flat and curved surfaces made of ferromagnetic steels. The usual procedure for in plane strain distribution determination requires manual placement and rotation of the BN probe on the sample and performing of the measurements at least for three different probe orientations [5]. In general one obtains this way the information about BN signal anisotropy which can be due to the other factors than only strain distribution [6]. This is a slow procedure, leads to accelerated damage of connecting cables and as a result one determines the strain distribution using the same 1D (strain vs BN intensity) calibration data for all directions. One can find information about the procedure of calibration curves normalization [7], yet it doesn't seem to be easily applicable for arbitrary directions of magnetization especially for anisotropic materials.

There have been proposed systems based on rotating magnetic field [8, 9] that were very sensitive to the materials

✉ Leszek Piotrowski  
lespiotr@pg.edu.pl

<sup>1</sup> Institute of Nanotechnology and Materials Engineering,  
Gdansk University of Technology, Narutowicza 11/12,  
80-233 Gdansk, Poland

anisotropy yet the issue of quantitative calibration of BN signal vs. stress was somewhat problematic. In those systems there is no defined magnetization direction as the field is being rotated continuously and stress/strain relation is more complicated. Both systems are based on mechanical rotation of permanent magnets what makes them difficult to miniaturize and requires relatively big flat area for the full rotation of the probe. In 2018 Kawai et al. proposed [10] a system with rotational field generated with the help of a three pole system yet it was overcomplicated and didn't draw much attention. The next step was multidirectional measurement system proposed later on [11]. The system used two perpendicular electromagnets for generation of magnetic fields oriented in any chosen direction that could be gradually rotated until the angular distribution of BN intensity was determined. Then the system calculated two strain components on the basis of two different calibration curves and determined the main strain axes orientation on the basis of the calibration curves interpolated for every measurement angle. The system worked very well for isotropic materials for which the interpolated curves were almost the same as the main ones. The problems occurred in case of materials for which the influence of normal (to magnetization direction) strain component was significant. It might be also noted that the abovementioned system could be easily adaptable to rotational BN measurements, simply by introducing a phase shift between magnetizing currents in perpendicular electromagnets.

There are two main goals of this work:

- Creation of the measurement set, that would be applicable to the anisotropic materials with no significant decrease of precision,
- Providing the end users with the system that can perform automatic calibration of the investigated material.

The first problem required a new algorithm of the strain determination procedure and to solve the second one it was necessary to build a robust, step motor driven, bending machine, capable of communication with measurement unit.

## 2 Strain/Stress Determination Procedure

The presented system is composed of two pieces of hardware, controlled by separate software, one of which is dedicated to strain generation and the other is responsible for BN signal measurements (the latter one can also work in a stand-alone mode). While working in calibration mode the system is controlled by the bending machine software, which handles communication between measurements unit and bending machine as well as between bending machine and a three

channel tensometric bridge used for automatic strain setting. The software uses only standard LabVIEW functions and DAQmx drivers, as for all the other procedures they are created by the authors.

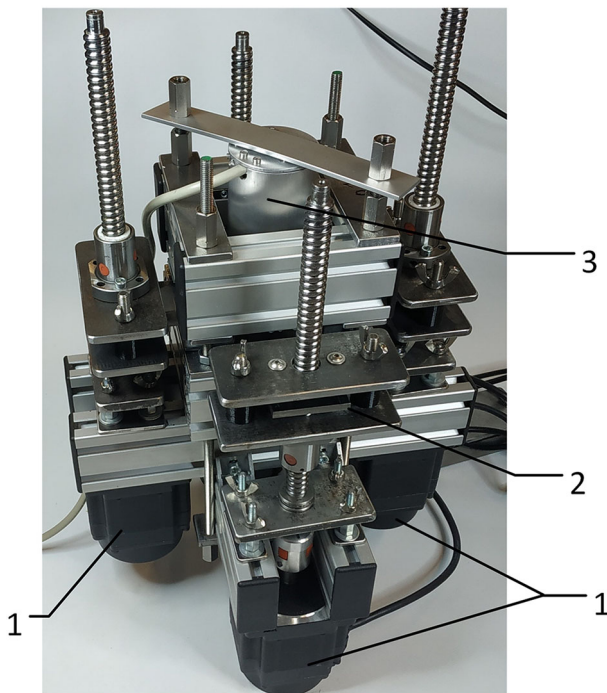
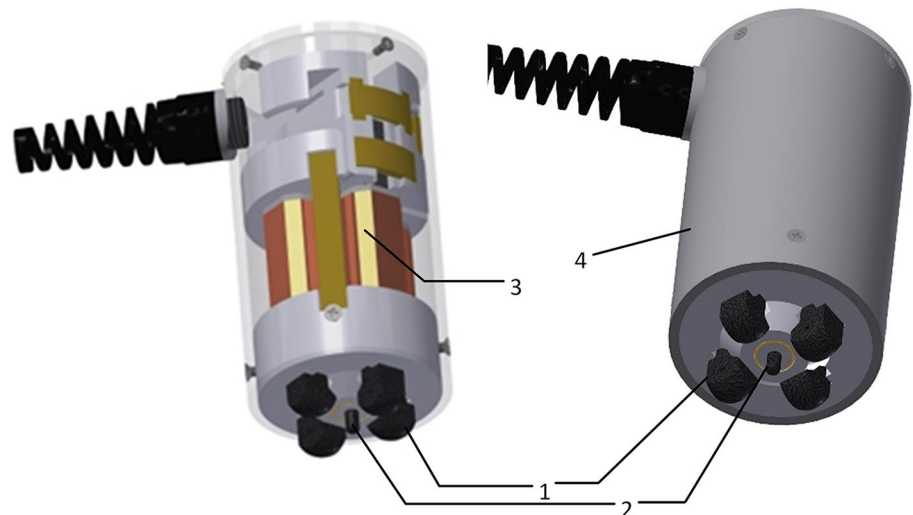
In the currently presented device a probe similar to the one described in [11] is applied for the determination of angular distribution of BN signal intensity—see Fig. 1. The probe consists of two c-core (1) electromagnets oriented in perpendicular directions. In the central point between the c-cores legs there is placed a pick up coil (2) with a ferritic core for the BN intensity determination. By the change of amplitudes of magnetizing currents in magnetizing coils (3) of both electromagnets one can set an arbitrary magnetization orientation in the point right below the pick-up coil. If the change is gradual one can rotate the magnetization by 360° and determine the BN signal angular distribution. The magnetizing current is triangular in form and its frequency and amplitude are adjustable. Typically the working frequency is about 10 Hz and magnetizing current amplitude is determined on the basis of the observed BN envelopes in such a way that one chooses the amplitude high enough to make the BN envelope values drop close to the background level. The signal for two half periods is measured and an average (after the reversal of the signal for decreasing magnetization) envelope is registered. Maximum current is 10A which, as it was shown with the help of finite element method (FEM) calculations, is high enough to produce, in common steels, the flux density of the order of 1–1.5 T in the material below the central point of the probe.

The device presented in this paper, having similar working principle of angular distribution of BN signal intensity measurement to the older one, boasts two features that make the described system truly unique. First of all the system is equipped with calibrating bending device, shown in Fig. 2, that can determine automatically calibration planes (BN intensity vs  $\epsilon_X$  and  $\epsilon_Y$ ) for two perpendicular directions with arbitrarily chosen strain step. The device is driven by four high torque step motors (1) that sets the required sample position.

During the calibration the system is controlled by the bending machine (calibrating device shown in Fig. 2) dedicated software which, manipulating cross shaped calibration sample (2) (moving the sample arms ends up and down in respect to its central part) produces required strain. Strain magnitudes and their accordance with main axes are controlled by three-axial resistance strain gauge (0°, 45°, 90°) connected via tensometric bridge with control unit. The 45° strain gauge direction is used for verification of sample mounting correctness. If the strains measured in perpendicular directions are truly main strains the intermediate gauge will show the value equal to their mean value. What is worth noting, the basic calibration procedure (i.e. maximum strain

**Fig. 1** BN measurement probe:

- 1—soft magnetic cores,  
2—detection coil (with ferritic core),  
3—magnetizing coils,  
4—shielding case

**Fig. 2** Calibrating device: 1—step motors, 2—calibrated sample; 3—BN measurement probe

$\varepsilon_{\max} = 600 \cdot 10^{-6}$ , strain step  $\Delta\varepsilon = 150 \div 200 \cdot 10^{-6}$ ) needs barely a few minutes to be performed.

The calibration process can be better understood with the help of a screenshot (see Fig. 3) taken during exemplary calibration run. In the right plot we can see values of strain  $\varepsilon_1$  (in blue) and  $\varepsilon_2$  (in red) already set during calibration. In the central part the indicator “matrix” shows the next target (strains to be set). The pre-set and obtained values of strain (current values of which (measured by tensometric bridge) are

displayed in the indicators “eps1” and “eps2”) are a bit different, depending on the value set by control “prec.” determining the strain setting procedure precision. The strain setting finishes when the value shown in “delta” indicator (sum of the absolute values of differences between pre-set and measured strains) is less than required precision. As soon as the setting ends, the calibration software sends the information to the measurement unit, triggers the measurement and waits for the measurement end signal. Together with the end signal the results of BN intensity measurements are sent back to the calibration software, stored and plotted in the “Int Ub” radial plot. In the case shown above one can see results obtained for the previous strain values—in that case  $\varepsilon_1 \approx 450 \cdot 10^{-6}$ ,  $\varepsilon_2 \approx 600 \cdot 10^{-6}$ . Every point in this plot represents the integral of the averaged BN signal envelope obtained for a given magnetization direction. Once the calibration is done the calibration planes are interpolated into a regular mesh.

Two dimensional calibration enables direct determination of true dependence of BN on strain state while, as should be noted a 1D calibration using tensile or bending machine neglects the influence of normal strain component. The influence of normal strain component on BN signal intensity have already been investigated both theoretically and experimentally in the 90’s [12]. At that time implementation of advanced 2D analysis in portable device was however out of the question and the easiest way to make use of 2D calibration data was to print them and analyze graphically. As can be imagined it was a time consuming solution.

The BN measurements are usually performed for 36 angles ( $10^\circ$  step) both in a calibration and measurement modes. If need be, the calibration step might be increased up to  $45^\circ$  yet usually it is kept the same in order to control the correctness of calibration process. As a measure of BN

**Fig. 3** The screenshot showing an example of a calibration process in progress

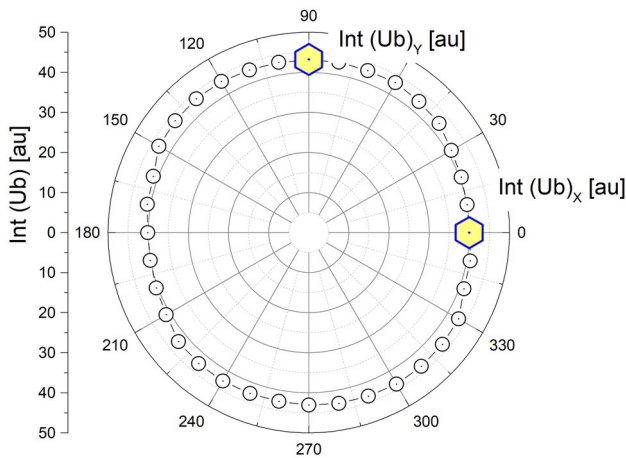
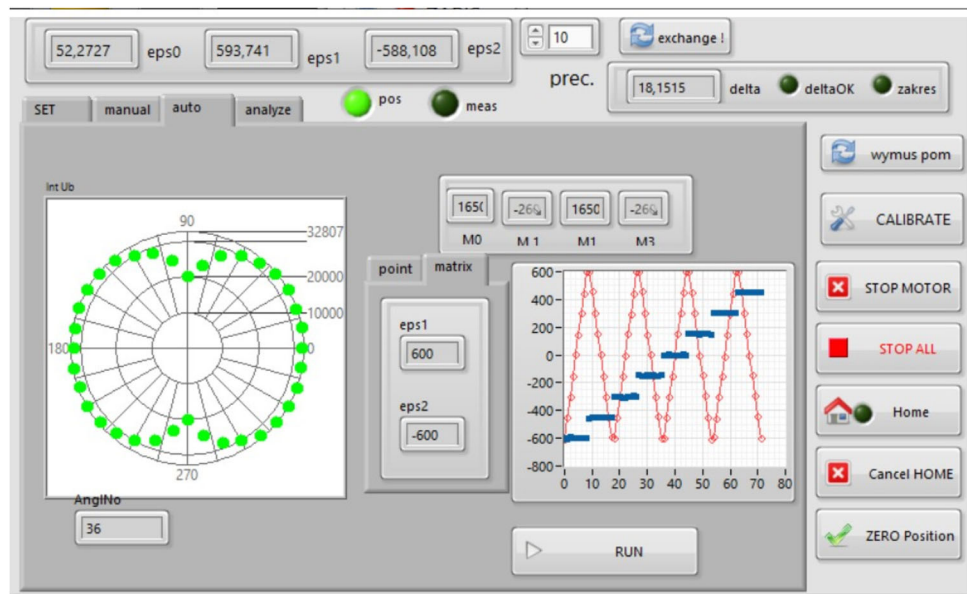


**Fig. 4** Example of angular distribution of BN intensity for the non-strained sample. Yellow hexagons indicate the values stored as calibration maps (Color figure online)

intensity we use the following formula (1):

$$Int(Ub) = \int_{(t=0)}^{(t=T/2)} \sqrt{(Ub_{raw}^2 - Ub_0^{(2)})} dt, \quad (1)$$

where  $Ub_{raw}$  is the envelope of the BN noise signal and  $Ub_0$  stands for a background noise level.

Figure 4 shows a typical angular distribution of the BN signal intensity—there are also marked the values that are recorded as calibration planes ( $Int(Ub)_x$  and  $Int(Ub)_y$ ). At the end of the calibration process two dimensional BN signal distributions are saved and the measurement set can be used independently. In the present version of the device both calibration surfaces are always taken into account. The example of calibration surfaces (for two perpendicular directions of

magnetization) are shown in Fig. 5. In order to illustrate the strain assessment process there is also plotted a horizontal plane representing the example of measured value. Crossing line of calibration surface and horizontal measurement plane indicate the best fitting values of a given strain components. Figures 6 and 7 show the differences ( $dX$ ,  $dY$ ) between measured signal and calibration surfaces.

Since we are looking for the two dimensional strain/stress distribution we have look for the point on the  $(\epsilon_x, \epsilon_y)$  plane for which both differences reach the smallest obtainable values. In order to do that we have to choose a function that will take into account both calibration planes in a similar way. In our case we decided to use as a figure of merit (FOM), i.e. the function that is to be minimized, the “distance” to both surfaces defined as:

$$dXY = \sqrt{dX^2 + dY^2}, \quad (2)$$

where  $dX$  and  $dY$  represent the abovementioned differences.

The obtained values of  $dXY$  are plotted in Fig. 8. A single, clearly visible minimum is obtained, indicating optimum strain components in both  $x$  and  $y$  directions. It may be observed that the  $dX$  and  $dY$  values do not represent the true distances to surfaces, as such should be calculated in a normal to surface direction instead of a vertical one. The minimization is performed in two steps—firstly the “distance” is calculated for every point of the calibration mesh and the minimum value is found. The strain components (coordinates of that point) are used as a starting point for the second stage. In that stage the minimum is searched using the algorithm that is probing the behavior of “distance” during the shift in four, normal directions.

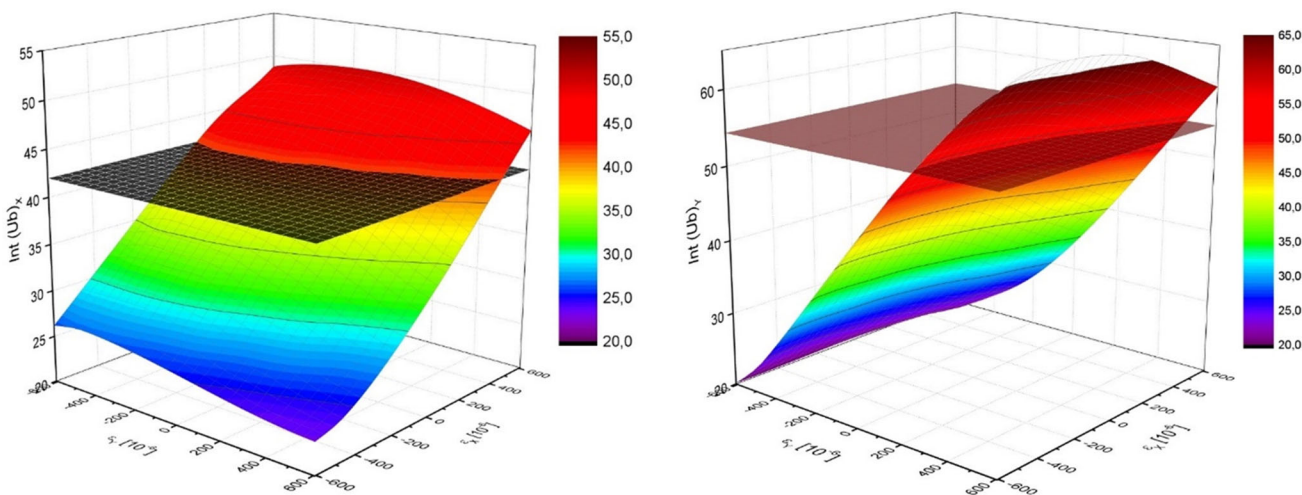


Fig. 5 Calibration surfaces for magnetization in x (left) and y (right) directions. Horizontal plane represents the single measurement result

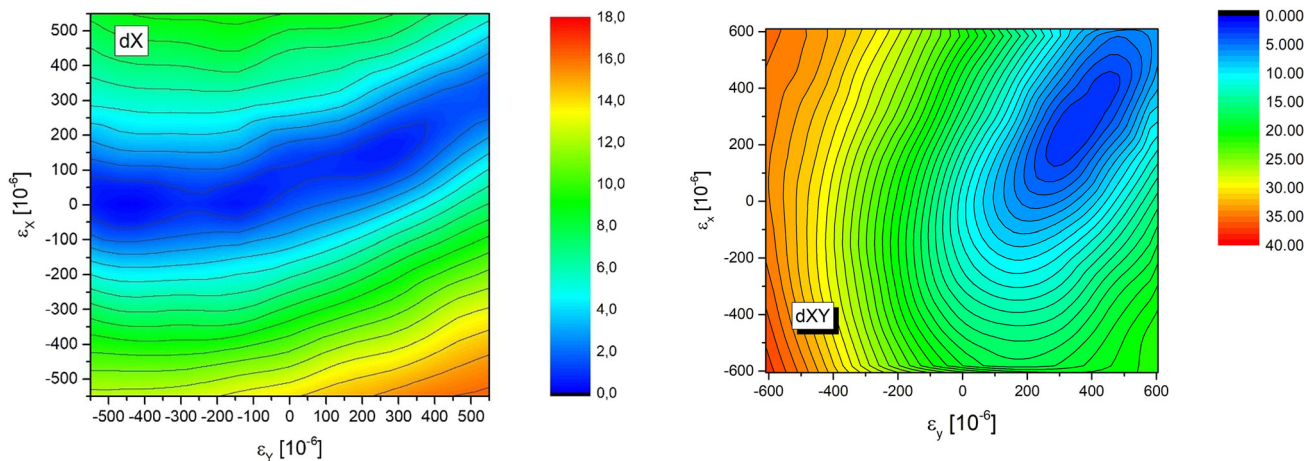


Fig. 6 Difference between the measured signal (x direction) and the appropriate calibration surface

Fig. 8 The “distance” from both calibration planes—clearly visible minimum indicates best match to strain components

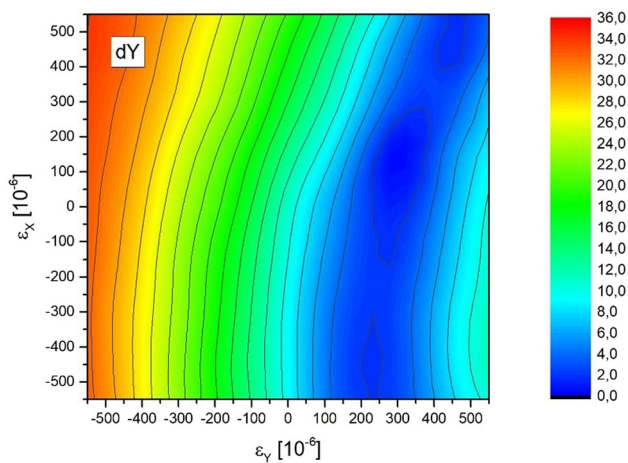
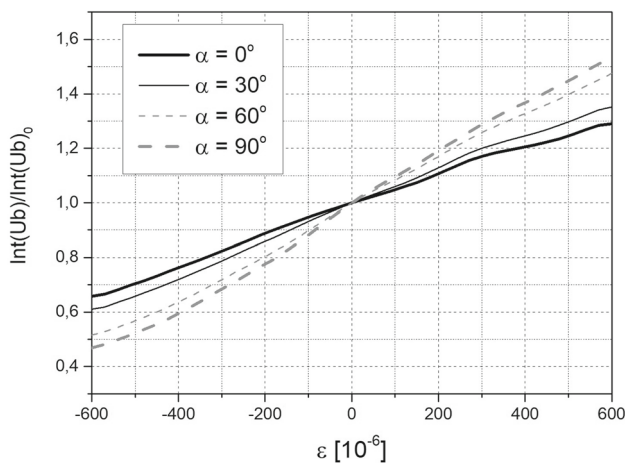


Fig. 7 Difference between the measured signal (y direction) and the appropriate calibration surface

If, for any direction, one observes a decrease then the starting point is shifted in the direction of the highest decrease and the procedure is repeated until the FOM drops below the acceptance level. If all probing attempts result in the increase of minimized function the distance is reduced until FOM reaches the predefined minimum value or the number of iterations is exceeded.

The algorithm described above is however applicable only for determination of X and Y components of strain and does not allow for the determination of main strain values and/or directions. Being so, the orientation of the main axes is obtained with the help of the angular distribution of the BN signal intensity (exactly in the same way as in the older device [11]). In order to find the main axes the calibration curves for X and Y directions are extracted from the calibration surfaces and on their basis the predicted curves for intermediate magnetization orientations are generated (assuming cosine



**Fig. 9** Additional calibration curves for intermediate magnetization direction orientations

squared like transition [11]). The example of such curves is shown in Fig. 9, where the normalized curves (measured values divided by the ones for zero strain values) for a sample made of S235JR steel are presented. Usually the normalized curves (and also maps) are used as they tend to be less environment dependent than absolute values, provided that we have the reference sample available, if no we have to use recorded reference data. The important feature of normalization procedure is that the normalized  $Int(Ub)$  distribution has usually roughly similar orientation as the main strain components allowing for a fast assessment of strain distribution e.g. on the surface of a welded plate.

Using such sets of calibration curves, in order to obtain main strain axis orientation one determines the angular strain distribution which is then fitted with function:

$$\varepsilon_\phi = \varepsilon_Y + (\varepsilon_X - \varepsilon_Y) \cos^2(\phi - \alpha), \quad (3)$$

where  $\alpha$  describes the main strain orientation in respect to OX axis.

Being so one gets a set of three parameters ( $\varepsilon_{\min}$ ,  $\varepsilon_{\max}$ ,  $\alpha$ ) which allows to unambiguously determine the main strain components:

$$\varepsilon_1 = \frac{\varepsilon_x \cos^2 \alpha - \varepsilon_y \sin^2 \alpha}{\cos 2\alpha} \quad (4a)$$

$$\varepsilon_2 = \frac{\varepsilon_y \cos^2 \alpha - \varepsilon_x \sin^2 \alpha}{\cos 2\alpha} \quad (4b)$$

The only problem with the formula is for the  $\alpha$  angles close to  $45^\circ$  as the denominator goes to zero. In such a case one can use less precise method and obtain the values of main strain components directly from the results of fitting of strain angular distribution. The following calculations, for stress state determination, can then be performed with the

help of the Hooke's law. The Young modulus and Poisson's ratio are assumed to be isotropic. This is a reasonable assumption since mechanical tests (tensile loading) didn't show any measurable mechanical anisotropy. The relations applied are as follows:

$$\sigma_1 = \frac{E}{1 - \nu^2} (\varepsilon_1 + \nu \varepsilon_2) \quad (5a)$$

$$\sigma_2 = \frac{E}{1 - \nu^2} (\varepsilon_2 + \nu \varepsilon_1) \quad (5b)$$

### 3 Experimental Verification of Strain Determination Precision

In order to verify the correctness of the assumptions regarding the proposed algorithms of both calibration and measurements we have performed a two stage experiment. The sample was cut out from a cold rolled sheet (Polish steel grade S460M) and displayed a noticeable BN signal anisotropy both regarding the initial values of BN intensity and their response to applied strain. In the first stage we have performed a calibration run on a arbitrarily selected sample and, after completion of the process, removed the probe and sample from the bending machine. In the second stage we placed them back and performed new calibration run, with different range and step of applied strain. This time we treated it as "measurement" and calculated the strain values on the basis of the registered BN signals.

The exemplary calibration results (first stage) are shown in Fig. 10 (BN intensity angular distribution) and Fig. 11 (BN intensity as a function of strain components for two perpendicular directions of magnetization). As can be seen from BN angular distribution, the influence of strain in direction perpendicular to the measurement direction is different for  $x$  (horizontal) and  $y$  (vertical) directions and contributes to BN signal anisotropy. For instance if we look at  $\varepsilon_x = -600 \cdot 10^{-6}$ ,  $\varepsilon_y = 0$  strain state (full squares) and analyze BN measurements in  $y$  direction ( $90^\circ$ ) the difference between intensity for the given and for the zero strain  $\varepsilon_x = \varepsilon_y = 0$  (empty circles) is negligibly small, so we can assume that the influence of normal strain component is small. On the other hand for  $\varepsilon_x = 0$ ,  $\varepsilon_y = -600 \cdot 10^{-6}$  (full diamonds) the difference is visible – the results for  $x$  direction ( $0^\circ$ ) are significantly higher in case of strained sample. In the case of tensile strain  $\varepsilon_x = 600 \cdot 10^{-6}$ ,  $\varepsilon_y = 0$  (empty squares) and  $\varepsilon_x = 0$ ,  $\varepsilon_y = 600 \cdot 10^{-6}$  (empty diamonds) the situation is different, as this time in both cases one observes the decrease of normal component ( $y$  and  $x$  respectively). The change is quite pronounced so one can expect strong influence of normal tensile strain on the results of BN intensity measurements. The results are confirmed by the calibration planes – one can observe  $Int(Ub)_y$

**Fig. 10** Angular distribution of the BN intensity for different strain components (x—horizontal, y—vertical direction)

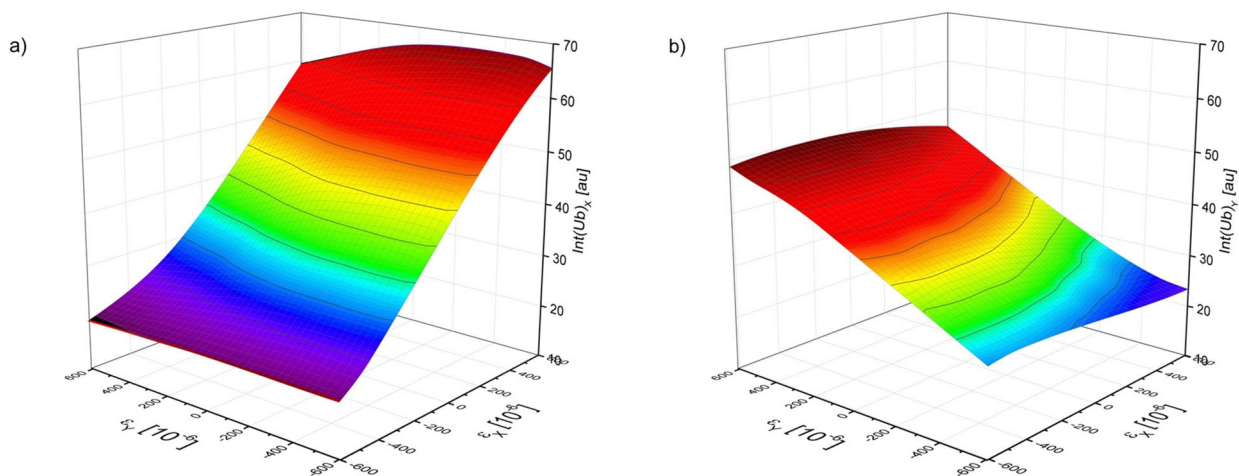
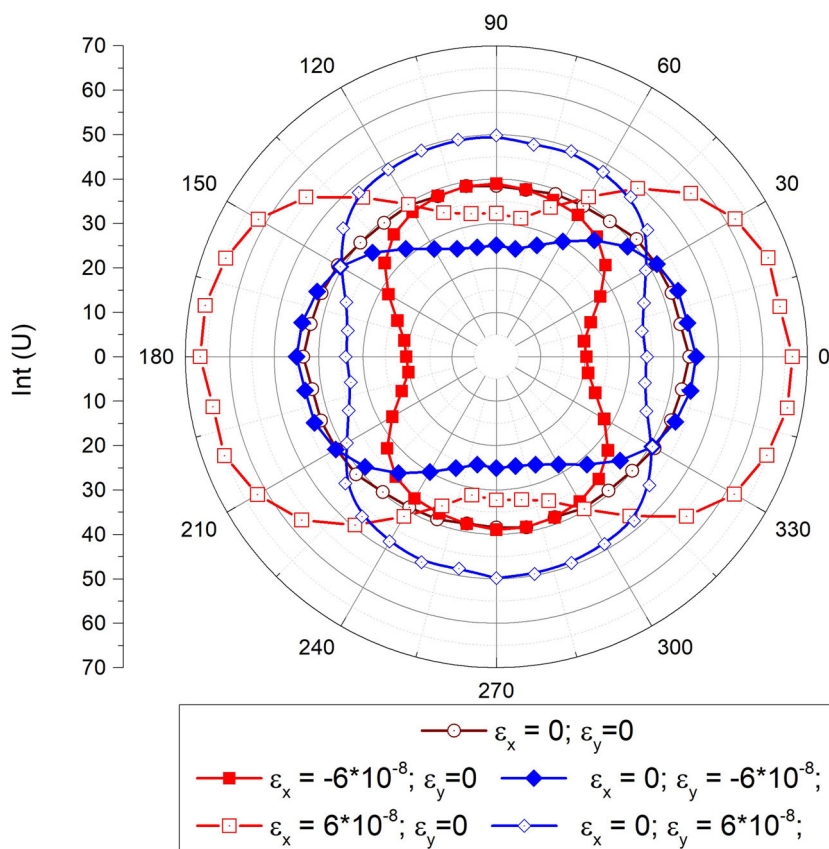


**Fig. 11** Calibration surfaces for S460M grade steel for two perpendicular magnetization directions: **a** x direction, **b** y direction

to be almost constant for negative values of  $\epsilon_x$ ,  $Int(Ub)_x$  to increase slightly for negative values of  $\epsilon_y$  and finally both the  $Int(Ub)_x$ ,  $Int(Ub)_y$  values decrease for increasing positive values of  $\epsilon_y \epsilon_x$ . It can be noted that the rate of change of BN signal intensity, as a function of y direction oriented strain, is about two times lower than for x direction. In such a case one can expect better accuracy of measurements in the latter direction. The “measurement” (calibration mode) run was performed for a set of strains, the most of which

did not coincide with original calibration strains. Since the automatic calibration run is possible only for equally spaced strains we have chosen a  $7 \times 7$  set of strains (49 strain levels in total) with maximum and step values  $450 \cdot 10^{-6}$  and  $150 \cdot 10^{-6}$  respectively for which only 9 are coincident with calibration set. The differences between measured strain components and the pre-set strains are shown in Figs. 12 and 13 (x and y components respectively). As it was predicted the average experimental error is significantly higher for y component

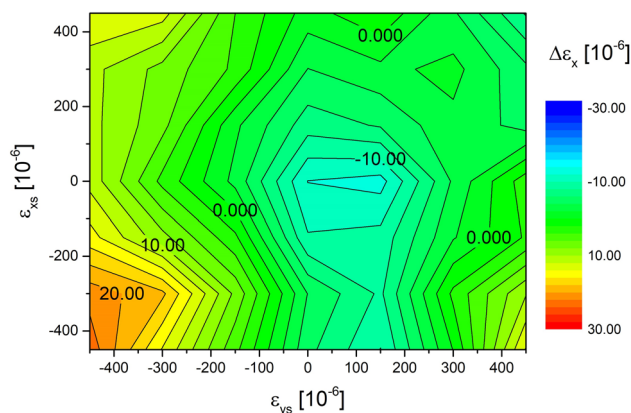


**Fig. 12** The differences ( $x$  components) between the measured and the pre-set strains ( $\varepsilon_{xs}$  and  $\varepsilon_{ys}$  stand for chosen pre-set components)

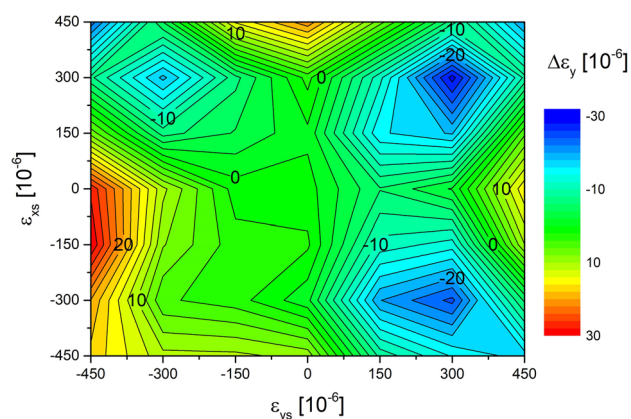


**Fig. 13** The differences ( $y$  components) between the measured and the pre-set strains ( $\varepsilon_{xs}$  and  $\varepsilon_{ys}$  stand for chosen pre-set components)

(up to  $30 \cdot 10^{-6}$  vs  $23 \cdot 10^{-6}$  in absolute values). In addition to that one can see that the obtained difference is not random (at least not completely) and some trends can be seen. One of the trends is the increase of error for  $45^\circ$  and  $135^\circ$  directions in the  $\varepsilon_x$ ,  $\varepsilon_y$  plane. This trend is more clearly visible for  $y$  direction, but it is observed also for the  $x$  one. Such a non-random error may suggest some kind of misalignment of the three important parts: bending machine, sample and measurement probe. The error is however relatively low and confirms the usefulness of the proposed system for the stress determination.

It should be stressed that measured values truly represent possible experimental error values since the control measurements were made after the removal of the probe from the calibration set and placing it again. If the probe is left mounted in the device the observed uncertainties are significantly smaller (repeatability of the BE signal intensity).

is good and standard deviation in such a case is typically of the order of 1%), but accuracy obtained this way would be overestimated and not obtainable in real life conditions.

## 4 Conclusions

The device described in the paper is the first BN measurement system available that can perform both automatic calibration and measurements. The fact that the strain measurement system is self-calibrating allows the end user to apply it for any chosen material, provided that he can get hold of material for calibration sample preparation. Thanks to its new algorithm of strain component determination, the apparatus can be applied for many different materials, both isotropic and anisotropic, even if the calibration planes are not fully monotonic. The differences between pre-set and measured strain values does not exceed  $30 \cdot 10^{-6}$  (resulting in stress evaluation error for steel about 6 MPa), what makes it comparatively accurate device. It can also be stressed that the described measurement procedure is both time and cost efficient allowing for automated control of, processing induced, strain/stress distribution over relatively big surfaces.

**Acknowledgements** This study was partly funded by Polish National Centre for Research and Development (Grant number POIR.01.01.01-00-1094/18-00).

**Author Contributions** Leszek Piotrowski: development of the software controlling the measurement/calibration sets, data processing, manuscript text preparation. Marek Chmielewski: design and construction of the measurement/calibration sets (hardware), calibration measurements, data processing.

**Data Availability** No datasets were generated or analysed during the current study.

## Declarations

**Conflict of interest** The authors declare no competing interests.

**Open Access** This article is licensed under a Creative Commons Attribution 4.0 International License, which permits use, sharing, adaptation, distribution and reproduction in any medium or format, as long as you give appropriate credit to the original author(s) and the source, provide a link to the Creative Commons licence, and indicate if changes were made. The images or other third party material in this article are included in the article's Creative Commons licence, unless indicated otherwise in a credit line to the material. If material is not included in the article's Creative Commons licence and your intended use is not permitted by statutory regulation or exceeds the permitted use, you will need to obtain permission directly from the copyright holder. To view a copy of this licence, visit <http://creativecommons.org/licenses/by/4.0/>.

## References

- Lu, J. (ed.): Handbook of Measurement of Residual Stresses. The Fairmont Press, Liburn (1996)
- Pasley, R.L.: Barkhausen effect—an indication of stress. Mater. Eval. **28**, 157–161 (1970)
- Rossini, N.S., Dassisti, M., Benyounis, K.Y., Olabi, A.G.: Methods of measuring residual stresses in components. Mater. Des. **35**, 572–588 (2012). <https://doi.org/10.1016/j.matdes.2011.08.022>



4. Santa-aho, S., Sorsa, A., Hakanen, M., Leiviska, K., Vippola, M., Lepisto, T.: Barkhausen noise-magnetizing voltage sweep measurement in evaluation of residual stress in hardened components *Meas. Sci. Technol.* **25**, 085602 (2014). <https://doi.org/10.1088/0957-0233/25/8/085602>
5. Capó-Sánchez, J., Pérez-Benitez, J., Padovese, L.R.: Analysis of the stress dependent magnetic easy axis in ASTM 36 steel by the magnetic Barkhausen noise. *NDT&E Inter.* **40**, 168–172 (2007). <https://doi.org/10.1016/j.ndteint.2006.12.009>
6. Palit, S.S., Ravi, K.B., Dobmann, G., Bhattacharya, D.K.: Magnetic characterization of cold rolled and aged AISI 304 stainless steel. *NDT&E Inter.* **38**, 674–681 (2005). <https://doi.org/10.1016/j.ndteint.2005.04.004>
7. Hristoforou, E., Vourna, P., Ktena, A., Svec, P.: On the universality of the dependence of magnetic parameters on residual stresses in steels. *IEEE Trans. Mag.* **52**(5), 6201106 (2016). <https://doi.org/10.1109/TMAG.2015.2509642>
8. Caldas-Morgan, M., Padovese, L.R.: Fast detection of the magnetic easy axis on steel sheet using the continuous rotational Barkhausen method. *NDT&E Inter.* **45**, 148–155 (2012). <https://doi.org/10.1016/j.ndteint.2011.10.003>
9. Ortega-Labra, O., Le Manh, T., Martinez-Ortiz, P., Hallen, J.M., Pérez-Benitez, J.A.: A novel system for non-destructive evaluation of surface stress in pipelines using rotational continuous magnetic Barkhausen noise. *Measurement* **136**, 761–774 (2019). <https://doi.org/10.1016/j.measurement.2019.01.018>
10. Kawai, A., Iida, S., Kasai, N.: Barkhausen noise measurement system using a three-pole probe. *J. Nondestruct. Eval.* **37**, 80 (2018). <https://doi.org/10.1007/s10921-018-0537-6>
11. Chmielewski, M., Piotrowski, L., Augustyniak, B.: A fast procedure of stress state evaluation in magnetically anisotropic steels with the help of a probe with adjustable magnetizing field direction. *Meas. Sci. Technol.* **28**, 045903 (2017). <https://doi.org/10.1088/1361-6501/aa5afb>
12. Augustyniak, B., Sablik, M.J.: The effect of mechanical stress on a Barkhausen noise signal integrated across a cycle of ramped magnetic field. *J. Appl. Phys.* **79**(2), 963–972 (1998). <https://doi.org/10.1063/1.360880>

**Publisher's Note** Springer Nature remains neutral with regard to jurisdictional claims in published maps and institutional affiliations.